British Journal of Pharmacology (2006) 148, 741–751 
www.nature.com/bjp

# *Grateloupia longifolia* polysaccharide inhibits angiogenesis by downregulating tissue factor expression in HMEC-1 endothelial cells

[1,2]Chao Zhang, [1,2]Fan Yang, *,[1]Xiong-Wen Zhang, [3]Shun-Chun Wang, [1,2]Mei-Hong Li, [1]Li-Ping Lin & *,[1]Jian Ding

[1]Division of Anti-Tumor Pharmacology, State Key Laboratory of Drug Research, Shanghai Institute of Materia Medica, Shanghai Institutes for Biological Sciences, Chinese Academy of Sciences, Shanghai, People's Republic of China; [2]Graduate School of the Chinese Academy of Sciences, Shanghai, People's Republic of China and [3]Institute of Chinese Materia Medica, Shanghai University of Traditional Medicine, Shanghai 201203, People's Republic of China

**1** The antiangiogenic and antitumor properties of *Grateloupia longifolia* polysaccharide (GLP), a new type of polysaccharide isolated from the marine alga, were investigated with several *in vitro* and *in vivo* models. Possible mechanisms underlying its antiangiogenic activity were also assessed.

**2** GLP dose-dependently inhibited proliferation of human microvascular endothelial cells (HMEC-1) and human umbilical vein endothelial cells (HUVEC), with $IC_{50}$ values of 0.86 and 0.64 mg ml$^{-1}$, respectively. In tube formation and cell migration assays using HMEC-1 cells, noncytotoxic doses of GLP significantly inhibited formation of intact tube networks and reduced the number of migratory cells. Inhibition by GLP was VEGF-independent.

**3** In the chick chorioallantoic membrane (CAM) assay, GLP (2.5 $\mu$g egg$^{-1}$) reduced new vessel formation compared with the vehicle control. GLP (0.1 mg plug$^{-1}$) also reduced the vessel density in Matrigel plugs implanted in mice.

**4** The levels of pan and phosphorylated recptors for VEGF, VEGFR-1 (flt-1) and VEGFR-2 (KDR) were not significantly altered by 5 mg ml$^{-1}$ GLP treatment of HMEC-1, although tissue factor (TF) showed significant decreases at both mRNA and protein levels following GLP treatment.

**5** In mice bearing sarcoma-180 cells, intravenous administration of GLP (200 mg kg$^{-1}$) decreased tumor weight by 52% without obvious toxicity. Vascular density in sections of the tumor was reduced by 64% after GLP treatment.

**6** Collectively, these results indicate that GLP has antitumor properties, associated at least, in part, with the antiangiogenesis induced by downregulation of TF.
*British Journal of Pharmacology* (2006) **148,** 741–751. doi:10.1038/sj.bjp.0706741;
published online 22 May 2006

**Keywords:** *Grateloupia longifolia* polysaccharide; antiangiogenesis; tissue factor; HMEC-1

**Abbreviations:** bFGF, basic fibroblast growth factor; CAM, chick chorioallantoic membrane; DMSO, dimethyl sulfoxide; dNTPs, deoxynucleoside triphosphates; ECGS, endothelial cell growth supplements; EGF, epidermal growth factor; ELISA, Enzyme-Linked Immunosorbent Assay; FBS, fetal bovine serum; GAPDH, glyceraldehyde-3-phosphatedehydrogenase; GLP, *Grateloupia longifolia* polysaccharide; HMEC-1, human microvascular endothelial cell; HUVEC, human umbilical vein endothelial cell; i.v., intravenous; MAPK, mitogen-activated protein kinase; M-MLV, Moloney murine leukemia virus; RT–PCR, reverse transcription–polymerase chain reaction; SRB, sulforhodamine B; TF, tissue factor; TUNEL, terminal deoxynucleotidyl transferase Biotin-dUTP nick end labeling; VEGF, vascular endothelial growth factor

## Introduction

Angiogenesis, which is the formation of new vessels from pre-existing microvascular networks, plays a crucial role in tumor progression (Folkman, 1990; Hanahan & Folkman, 1996). In cancer, new vessel formation contributes to the progressive growth and metastasis of solid tumors (Liotta *et al*., 1991), making antiangiogenesis an important strategy in cancer therapeutics. Avastin (bevacizumab), a humanized monoclonal antibody against vascular endothelial growth factor (VEGF), was approved by the FDA for clinical use as the first tumor angiogenesis inhibitor (TAI) in 2004. It is now widely accepted that the angiogenic switch is 'off' when the effects of pro- and antiangiogenic molecules are balanced, and 'on' when the net balance tips in favor of angiogenesis (Bouck *et al*., 1996; Hanahan & Weinberg, 2000). Given that the proangiogenic factors such as VEGF (Neufeld *et al*., 1994), basic fibroblast growth factor (bFGF) (Fahmy *et al*., 2003), epidermal growth factor (EGF) (Kos & Dabrowski, 2002) and tissue factor (TF) (Rickles *et al*., 2003) are essential for triggering the angiogenic cascades, targeting proangiogenic factors is becoming an attractive approach for the prevention of tumor-associated angiogenesis.

*Authors for correspondence; X.-W. Zhang,
E-mails: xwzhang@jding.dhs.org or J. Ding,
J Ding; jding@mail.shcnc.ac.cn

We have sought to identify potential inhibitors of angiogenesis and anticancer compounds from natural marine resources, which are a rich source of new chemical diversity and potential therapeutic drug leads. *Grateloupia longifolia* polysaccharide (GLP) is a new type of polysaccharide isolated from the alga *G. longifolia* which is widely distributed in inshore areas of China, Namibia, Australia and New Zealand (Guiry & Nic Dhonncha, 2000). Here, using a range of assays, we found that GLP has antiangiogenic and antitumor activities both *in vitro* and *in vivo*. Analysis of the mechanisms of its actions indicated that suppression of TF could contribute to its antiangiogenic action.

## Methods

### *Animals and cell lines*

The use of animals was approved by the Institute animal reviews boards of Shanghai Institute of Materia Medica, Chinese Academy of Sciences, with firm adherence to the ethical guidelines for the care and use of animals. Specific pathogen-free (SPF) female KM mice (7-week-old, 18–22 g) were provided by Shanghai Laboratory Animal Center, Chinese Academy of Sciences. C57BL/6J mice (7-week-old, 16–18 g) were from Laboratory Animal Center, Shanghai Institute of Materia Medica, Chinese Academy of Sciences.

The human microvascular endothelial cell line HMEC-1 was obtained from the American Type Culture Collection (ATCC, Manassas, VA, U.S.A.) and propagated in MCDB131 supplemented with 20% fetal bovine serum, 30 $\mu$g ml$^{-1}$ endothelial cell growth supplements (ECGS), 10 ng ml$^{-1}$ epithelial growth factor (EGF) and 1 $\mu$g ml$^{-1}$ hydrocortisone. Human umbilical vein endothelial cells (HUVEC) were isolated from human umbilical cord veins by 0.1% type-I collagenase digestion at 37°C for 15 min and their identity confirmed by immunofluorescence using anti-von Willebrand factor antibody. HUVECs were maintained in M199 culture medium with 20% FBS, 30 $\mu$g ml$^{-1}$ ECGS, and 10 ng ml$^{-1}$ EGF, and used at passages 3–7. Human gastric cancer cell line MKN-28 (Japanese Foundation for Cancer Research), human colon cancer cell line HCT-116 (National Cancer Institute, U.S.A.), human breast carcinoma cell line MDA-MB-435, human ovary cancer cell line SK-OV-3, mouse fibroblast cell line NIH-3T3 (ATCC), and mouse S-180 sarcoma cell line (Shanghai Institute of Materia Medica, Chinese Academy of Sciences) were maintained in RPMI-1640 medium supplemented with 10% FBS, penicillin (100 IU ml$^{-1}$) and streptomycin (100 $\mu$g ml$^{-1}$). All cells were cultured in a highly humidified atmosphere of 5% $CO_2$ at 37°C.

### *Extraction and characterization of GLP*

Fresh *G. longifolia* (1 kg) was extracted with 5 l water (buffered at pH 6.0 with acetic acid) at 90°C for 30 min. The mixture was centrifuged at 900 × *g* for 20 min, and the pellet was re-extracted as above. The supernatant fractions were combined, centrifuged at 2500 × *g* for 10 min, dialyzed against distilled water for 2 days, and then mixed with four volumes of acetone. The precipitate was dissolved in distilled water, and then freeze-dried to yield ~110 g of GLP. The molecular weight of the polysaccharide was estimated to be 1000 ± 100 kDa based on a high-performance liquid chromatography-gel permeation chromatography analysis. Sugar composition analysis showed that the polysaccharide was composed of 3,6-anhydrous-galactose, 6-methyl-galactose, 2-methyl-galactose and galactose in the molar ratios of 0.96 : 0.35 : 0.05 : 7.48. The sulfate content was 18.5%, as assessed by gelatin-barium chloride assay. Methylation analysis results showed that the polysaccharide contained 1,4 linked 3,6-anhydrous-galactose, 1,3 linked galactose, 1,4 linked galactose, 1,2,4 linked galactose, 1,2,3 linked galactose, 1,3,6 linked galactose and 1,4,6 linked galactose. For *in vitro* assays, GLP was dissolved in complete cell culture medium or serum-free MCDB 131 (GIBCO Green Island, NY, U.S.A.) culture medium. For *in vivo* assays, GLP was dissolved in normal saline (NS).

### *Sulforhodamine B assay*

The growth inhibition effect of GLP on various cell and cell lines was examined with the sulforhodamine B (SRB) assay (Tan *et al*., 2003). Briefly, HMEC-1, HUVEC, MDA-MB-435, MKN-28, HCT-116, SK-OV-3 and NIH-3T3 cells were seeded in 96-well plates at densities indicated by our previous experiments. After incubation overnight, triplicate wells were treated with various concentrations of GLP. After 12 or 72 h, the culture medium was discarded, 10% (w v$^{-1}$) precooled (4°C) trichloroacetic acid (100 $\mu$l) was added to each well, and the cells were fixed at 4°C in a refrigerator for 1 h. Each well was then stained with 100 $\mu$l 0.4% SRB (w v$^{-1}$) in 1% acetic acid (v v$^{-1}$) for 15 min. The plates were washed with 1% acetic acid (v v$^{-1}$) for removal of unbound dye, air dried, and then treated with 150 $\mu$l well$^{-1}$ 10 mM Tris base (pH 10.5) to dissolve the bound dye. The absorbance in each well was read with a multiwell spectrophotometer (VERSAmax, Molecular Devices, Union City, CA, U.S.A.) at 515 nm. The inhibition of cell proliferation was computed as $[1-(A_{515\ \text{treated}} \cdot A_{515\ \text{control}}{}^{-1})] \times 100\%$, and the $IC_{50}$ (concentration for 50% inhibition) was calculated by the Logit method.

For the assay of cell proliferation stimulated by VEGF, HMEC-1 cells ($5 \times 10^3$ cells well$^{-1}$) were seeded to 96-well plates in MCDB 131 (with 20% FBS). After attachment overnight, HMEC-1 were starved in MCDB131 with 1% FBS for 24 h. After being washed with phosphate-buffered saline three times, the cells in fresh MCDB131 with 1% FBS or 20% FBS were preincubated with different concentrations of GLP for 1 h before the addition of 20 ng ml$^{-1}$ VEGF (to 1% FBS group) or VEGF vehicle (to 20% FBS group). After incubation for 72 h, the number of cells was estimated by the SRB assay. Inhibition of cell proliferation was computed as $[1-(A_{515\ \text{treated}} \cdot A_{515\ \text{control}}{}^{-1})] \times 100\%$.

### *ELISA for incorporation of BrdU*

Quantification of BrdU incorporation during DNA synthesis in proliferating cells was an index of cell viability (Hawker, 2003). ELISA for BrdU incorporation was performed according to the instruction manual (Roche Diagnostics, Mannheim, Germany). Briefly, after HMEC-1 were exposed to various concentrations of GLP for 8 h in 96-well plate, 10 $\mu$l BrdU labeling solution was added to each well and incubated for another 4 h. Then labelling medium was removed and 200 $\mu$l FixDenat solution added to each well at room temperature for 30 min. The FixDenat solution was then discarded and 100 $\mu$l

anti-BrdU-POD working solution incubated with the cells at room temperature for 90 min. After washing each well three times with 300 $\mu$l washing solution, 100 $\mu$l substrate solution was added and kept at room temperature for 20 min. 25 $\mu$l 1 M $H_2SO_4$ was used to stop the reaction. The absorbance was read by a multiwell spectrophotometer at 450 nm. The relative growth rate was computed as: $(A_{450\ \text{treated}} \cdot A_{450\ \text{control}}{}^{-1}) \times 100\%$.

### *Terminal deoxynucleotidyl transferase mediated dUTP-biotin nick end-labeling*

The terminal deoxynucleotidyl transferase mediated dUTP-biotin nick end-labeling (TUNEL) assay was performed with the *In Situ* Cell Death Detection Kit (Roche Diagnostics), according to the manufacturer's instructions. Briefly, after treatment with GLP or VP-16 (a known inducer of apoptosis: Shimizu *et al*., 1990) for 12 h, the cells growing on slides in six-well plate were fixed in 4% paraformaldehyde, permeabilized with 0.1% Triton X-100 and 0.1% sodium citrate (freshly prepared), and labeled with fluorescein- 12-dUTP. Apoptosis was detected by fluorescence microscopy (Olympus, BX51, Japan).

### *Cell migration assay*

The migration ability of HMEC-1 was tested in a Transwell Boyden Chamber (Costar, Bethesda, MD, U.S.A.) using a polycarbonate filter (8 $\mu$m pores) and a 0.1% gelatin matrix in the upper chamber. In the standard assay, 100 $\mu$l of cell suspension ($10^6$ cells ml$^{-1}$) in serum-free MCDB 131 culture medium (vehicle) with GLP or vehicle (control) was added to the upper chamber, while the lower chamber contained 600 $\mu$l MCDB131 with 20% FBS or MCDB 131 with 20 ng ml$^{-1}$ VEGF supplemented with the same concentration GLP or vehicle. The apparatus was incubated for 8 h at 37°C, and then the upper chambers were disassembled and fixed with 90% ethanol. The membranes were stained with 0.1% crystal violet in 0.1 M borate and 2% ethanol for 15 min (Sheu *et al*., 1998). Cells remaining on the upper surface of the filter membrane (nonmigrant) were scraped off gently with a cotton swab. Images of migrant cells were captured by a photomicroscope (Olympus, BX51, Japan). Stained cells were extracted with 100 $\mu$l 10% acetic acid, and the absorbance was measured at 600 nm using a multiwell spectrophotometer with the value from the lower chamber set as zero absorbance. Inhibition of cell migration was computed as $(1-(A_{600\ \text{treated}} \cdot A_{600\ \text{control}}{}^{-1})) \times 100\%$.

### *Tube formation assay*

A tube formation assay was used to investigate the effect of GLP on angiogenesis *in vitro*. A 96-well plate was coated with 60 $\mu$l liquid Matrigel per well, which was allowed to solidify at 37°C for 45 min. HMEC-1 were seeded at a density of $3 \times 10^4$ cells well$^{-1}$ in 100 $\mu$l complete culture medium containing different concentrations of GLP (5, 2.5, 1.25, 0.625 and 0.313 mg ml$^{-1}$) or vehicle (control). Plates were incubated for 8 h at 37°C and 5% $CO_2$ (sufficient for formation of an intact network in the control group). Images were recorded by an inverted phase contrast microscope (Olympus, IX71, Japan), and tubes forming intact networks were counted.

### *Chick allantoic membrane assay*

The chick allantoic membrane (CAM) assay was carried out essentially as described by Tanaka *et al*. (1986). Fertilized eggs were incubated in a humidified egg incubator (Lyon, Chula Vista, CA, U.S.A.) for 7 days. On the 8th day, a small orifice was made on the broad side of the egg and a window was carefully created through the egg shell. Squares of Whatman filter paper ($5 \times 5$ mm) were soaked with 5 $\mu$l of normal saline containing 2.5–50 $\mu$g GLP and then implanted on the CAM. Suramin (7.2 $\mu$g egg$^{-1}$ (5 nmol egg$^{-1}$)) similarly applied served as a positive control. The windows were sealed with adhesive tape and the eggs were incubated for another 48 h, during which time nonviable eggs were discarded. Initially, 15 eggs were tested for each concentration (control, GLP and suramin) to ensure that at least 10 viable embryos were assessed. The zones of neovascularization under and around the filter paper were photographed using an anatomic microscope (Leica, MS5, Switzerland) and pictures were printed out as $5 \times 7$ in$^2$ prints. Vessel branches $<3$ mm long in five random $1 \times 1$ in$^2$ zones per picture were counted and five eggs were chosen from each group. Inhibition was computed as $(1-(\text{branches}_{\text{treated}} \cdot \text{branches}_{\text{control}}{}^{-1})) \times 100\%$.

### In vivo *Matrigel plug assay*

An *in vivo* Matrigel plug assay was carried out as described earlier (Akhtar *et al*., 2002). Precooled liquid Matrigel (500 $\mu$l containing 100 ng bFGF added) with or without GLP was subcutaneously injected into the midventral abdominal region of 7-week-old C57BL/6J mice. At 5 days postinjection, 200 $\mu$l dextran-FITC (dissolved in saline, 20 mg ml$^{-1}$) was injected through the tail vein. After 5 min later, mice were killed and the Matrigel plug was removed, carefully separated from the subcutaneous tissues and muscles, and fixed in 4% formalin dissolved in PBS. Pictures were captured by fluorescent microscopy (Olympus, BX51, Japan). We used Abobe® Photoshop to quantitate the fluorescence of different groups. All pictures were captured in an RGB 8-bit format (24-bit red, green, blue). We analyzed the 8-bit green band in Adobe® Photoshop 7.0, and the results were indicated by histograms and mean values ($\pm$s.d.) computed by Photoshop.

### *Real-time reverse transcription–polymerase chain reaction assay*

After exposure to various concentrations of GLP (0.2, 1, 5 mg ml$^{-1}$) and vehicle (HMEC-1 culture medium) for 24 h, HMEC-1 ($5 \times 10^5$ cells ml$^{-1}$) were harvested and total mRNA was isolated using the TRIzol reagent (Bio Basic Inc., Markham Ontario, Canada) according to the manufacturer's instructions. RNA yields and purity were assessed by spectrophotometric analysis. Total RNA (1 $\mu$g) from each well was subjected to reverse transcription with random hexamer primers, deoxynucleoside triphosphates (dNTPs), and Maloney murine leukemia virus (M-MLV) reverse transcriptase in a total reaction volume of 20 $\mu$l. The synthesized cDNA was used immediately for real-time PCR amplification using primers specific for TF (sense, 5′-GAA GCA GAC GTA CTT GGC ACG G-3′; antisense, 5′-CCG AGG TTT GTC TCC AGG TA-3′) or the control glyceraldehyde-3-phosphate dehydrogenase (GAPDH; sense, 5′-GAA GGT GAA GGT

CGG AGT CA-3′; antisense, 5′-GAA GAT GGT GAT GGG ATT TC-3′). The real-time PCR reactions (20 $\mu$l) consisted of 2 $\mu$l PCR reaction buffer (Shanghai Sangon, Shanghai, China), 1 $\mu$l 10 mM dNTPs, 1 $\mu$l mixed primers (300 nM), 1 $\mu$l Taq polymerase, 1 $\mu$l cDNA, 1 $\mu$l SyBR green-I dye and 13 $\mu$l double-distilled water. Real-time PCR was carried out with the DNA Engine OPTICON 2 continuous fluorescence detector (MJ Research, Waltham, MA, U.S.A.). The results were semiquantitated using the equation: $Copy_{TF}:Copy_{GAPDH} = 2C(t)_{GAPDH} - C(t)_{TF}$. All PCR products were analyzed by electrophoresis on a 1.5% agarose gel, visualized with ethidium bromide, and analyzed using the Genesnap 6.00.26 software (Syngene, Cambridge, U.K.). Densitometric analysis was performed using GeneTools Analysis Software Version 3.02.00 (Syngene).

### *Western blot analysis*

The VEGF receptors, VEGFR-1 and VEGFR-2 are also called the flt-1 and KDR proteins. To detect these proteins in HMEC-1, cells in six-well plates were starved overnight, and then treated with different concentrations of GLP or vehicle for 2 h. VEGF (50 ng ml$^{-1}$) was used to stimulate the phosphorylation of VEGF-receptors. For detection of TF, HMEC-1 was treated with different concentrations of GLP or vehicle in six-well plates for 24 h. After the treatment procedures, trypsinized cells ($\sim 10^6$) were collected by centrifugation at 900 × *g* for 3 min, washed twice with precooled PBS, and then resuspended in lysis buffer (20 mM pH 7.5 Tris, 150 mM NaCl, 1 mM EDTA, 1 mM EGTA, 1% Triton X-100, 2.5 mM sodium pyrophosphate, 1 $\mu$g ml$^{-1}$ leupeptin, 1 mM PMSF and 10 $\mu$g ml$^{-1}$ aprotinin) on ice for 1 h. The lysates were centrifuged at 15,000 × *g* for 15 min at 4°C, and equivalent amounts of protein were resolved by 10% SDS–PAGE. After electrophoresis, the proteins were transferred onto nitrocellulose membranes (Millipore, Billerico, MA, U.S.A.), which were then blocked in blocking solution (5% nonfat milk in TBS/Tween) and incubated overnight at 4°C with antibodies against phosphorylated-KDR (1:1000), pan-KDR (1:1000), phosphorylated-flt-1 (1:1000), pan-flt-1 (1:1000), TF (1:5000) or $\beta$-actin (1:1000). Proteins were reacted with a peroxidase-coupled secondary antibody, which was then detected with ECL-plus. Densitometric analysis was performed with GeneTools Analysis Software Version 3.02.00 (Syngene).

### *Antitumor activity* in vivo *and tumor angiogenesis inhibition assay*

Seven-week-old specific pathogen-free (SPF) female KM mice were subcutaneously inoculated with S-180 sarcoma cells (4.0–6.5 × 10$^6$ cell mouse$^{-1}$) into the right armpit. After 24 h, daily treatments with GLP ($n = 8$) or saline ($n = 16$) were given by i.v. injection for 7 days, after which time animals were killed by cervical dislocation, and solid tumors were removed and weighed. Inhibition was calculated as ((Average tumor weight of NS group – Average tumor weight of test group). Average tumor weight of NS group$^{-1}$) × 100%.

The sarcoma 180 tumor specimens were separated from muscle and fixed in 10% formalin, and then paraffin embedded for immunofluorescent analysis. The paraffin embedded tumor sections (9-$\mu$m-thick) were dewaxed by washing in xylene and rehydrated through a graded series of ethanol and TBS washes. Antigen retrieval was carried out in citrate buffer (0.01 M, pH 6.0) heated by a medical microwave at 92–98°C for 15 min, then allowed to cool to room temperature, spontaneously. The slides were washed with TBS and permeabilized with 0.1% Triton X-100. Samples were incubated for 30 min at room temperature with a protein-blocking solution consisting of TBS and 3% bovine serum albumin. Excess blocking solution was removed, and the samples were incubated for 1 h at room temperature with a 1:300 dilution of rabbit anti-mouse CD31 polyclonal antibody. The samples were then rinsed with PBS and incubated for 60 min at room temperature with the appropriate dilution of Alexa Fluor® 488 chicken anti-rabbit IgG (H + L). All fluorescence photographs were taken under Olympus BX51 fluorescent microscope (Olympus, Japan). The same quantification method was applied as described for the *in vivo* Matrigel plug assay above.

### *Materials*

M199 medium, MCDB131 medium, RPMI-1640 medium and fetal bovine serum (FBS) were purchased from GIBCO (Grand Island, NY, U.S.A.). Endothelial cell growth supplement (ECGS) and Matrigel™ were from Beckon Dickinson Labware (Bedford, MA, U.S.A.). Vascular endothelial growth factor (VEGF), epidermal growth factor (EGF), sulforhodamine B (SRB), basic fibroblast growth factor (bFGF), suramin, hydrocortisone and dextran-FITC (2000 kDa) were from Sigma (St Louis, MO, U.S.A.). The cell proliferation ELISA, BrdU (colorimetric) kit was from Roche Diagnostics GmbH, Roche Applied Science (Nonnenwald 2, Penzberg, Germany). The goat polyclonal anti-human tissue factor antibody was from American Diagnostics Inc. (Stamford, CT, U.S.A.), while the rabbit polyclonal anti-human flt-1 and the goat polyclonal anti-human $\beta$-actin were from Santa Cruz Biotech (Santa Cruz, CA, U.S.A.). The rabbit polyclonal anti-phosphorylated human flt-1 was from Oncogene (Cambridge, MA, U.S.A.) while the rabbit polyclonal anti-human KDR and antiphosphorylated KDR were obtained from Cell Signaling Technology (Beverly, MA, U.S.A.). Finally, the rabbit anti-goat IgG (H + L) peroxidase-coupled secondary antibody was from Southern Biotech (Birmingham, U.K.), and the ECL-plus Western blotting detection system was from Amersham Biosciences (U.K.). The rabbit anti-mouse CD31 was from Boster Biological Technology Co., Ltd. (Wuhan, China). The Alexa Fluor® 488 chicken anti-rabbit IgG (H + L) was from Molecular Probes (Eugene, Oregon, U.S.A.). The TRIzol reagent was from Bio Basic Inc., Markham Ontario, Canada. Random hexamer primers from Shanghai Sangon, Shanghai, China. Deoxynucleoside triphosphates (dNTPs) and Maloney murine leukemia virus (M-MLV) reverse transcriptase from MBI (Hanover, MD, U.S.A.). SyBR green-I dye from Roche, Switzerland.

### *Data analysis*

The mean values were obtained from at least three independent tests. The data are presented as means ± s.d. and compared by ANOVA. The significance of differences between two concentration groups was computed by Bonferroni test.

$P<0.05$ was taken as significance of difference. The inhibition of tumor growth (as weights of the tumor tissue) was assessed by Student's *t*-test.

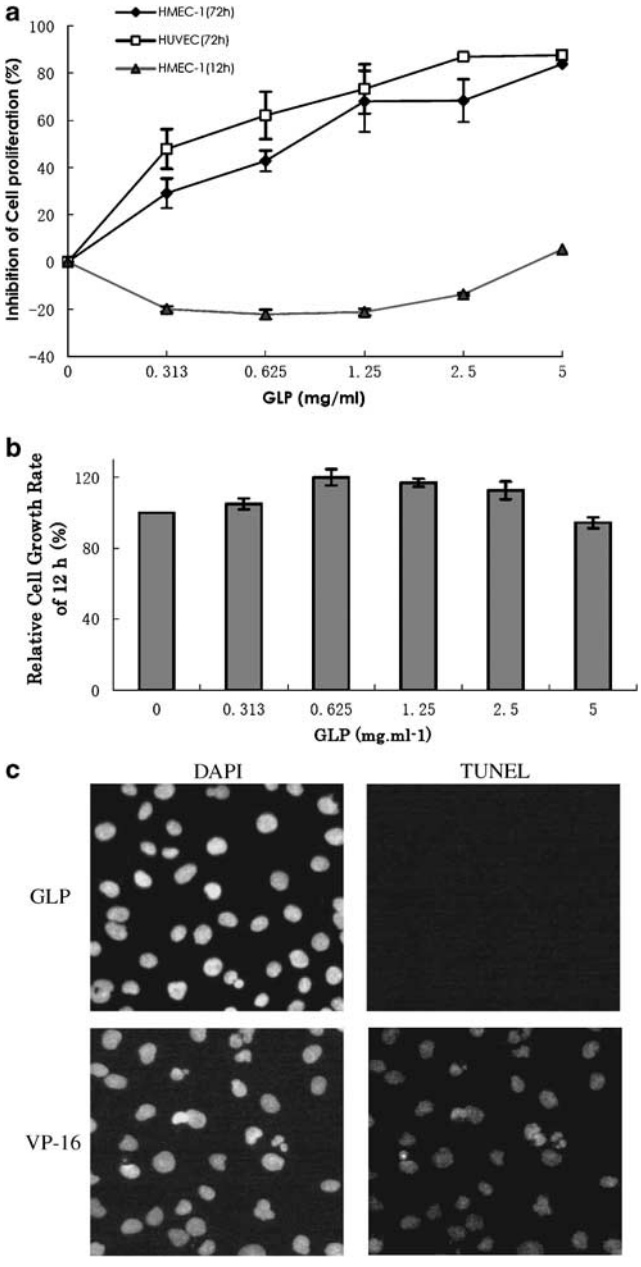


## Results

### *GLP inhibits cell proliferation*

We found that GLP dose-dependently inhibited the proliferation of HMEC-1 and HUVEC, with $IC_{50}$ values of 0.86 and 0.64 mg ml$^{-1}$, respectively (Figure 1a). GLP treatment also inhibited the growth of a variety of tumor and fibroblast cell lines and the mean $IC_{50}$ values for these cells are given in Table 1. The $IC_{50}$ values indicated that endothelial cell lines appeared to be more GLP-sensitive than tumor cell lines.

We also tested the effect of short-term incubations (12 h) with GLP on HMEC-1 cell viability by SRB, BrdU incorporation and TUNEL assays. The SRB assay demonstrated no inhibition of cell proliferation by GLP, over a range of concentrations below 5 mg ml$^{-1}$ (Figure 1a; see also 1c). The BrdU assay indicated that treatment of HMEC-1 with the same concentrations of GLP inhibited cell DNA synthesis very slightly; the highest concentration of GLP (5 mg ml$^{-1}$) decreased the relative cell growth rate by $<5\%$ (Figure 1b). The lack of a cytotoxic effect of GLP treatment, over 12 h, was also confirmed by the TUNEL assay. Treatment of HMEC-1 with 5.0 mg ml$^{-1}$ GLP for 12 h did not induce cell apoptosis, however, VP-16 (5 $\mu$M), as a positive control, induced significant DNA fragmentation. Green fluorescence illustrated the DNA nick (Figure 1c). The effect of 12 h incubation with 5.0 mg ml$^{-1}$ GLP on the other cell lines is shown in Table 1 and confirms the low toxicity of GLP towards these cells.

From these experiments we concluded that GLP at concentrations below 5 mg ml$^{-1}$ did not alter HMEC-1 viability over 12 h. Therefore, the investigations of antiangiogenic effects on HMEC-1 cells would be carried out at GLP concentrations of $<5$ mg ml$^{-1}$ and for an exposure time of $<12$ h.

**Figure 1** Suppression of cell proliferation by GLP. HMEC-1, HUVEC and tumor cells seeded in 96-well plates were treated with different concentrations of GLP for 72 h. Cell proliferation was measured by the SRB assay. (a) Inhibition over 72 h increased in a dose-dependent manner for both endothelial cell lines. Over 12 h (lowest line) GLP inhibited HMEC-1 proliferation very slightly, even at 5 mg ml$^{-1}$. (b) BrdU incorporation into HMEC-1 was not decreased after 5 mg ml$^{-1}$ GLP treatment for 12 h. (c) TUNEL assay showed 5 mg ml$^{-1}$ GLP did not induce apoptosis in HMEC cells over 12 h; however, 5 $\mu$M VP-16 induced significant apoptosis. DAPI (blue) showed nucleus, FITC (green) labeled DNA nick (100-fold amplification). The mean of triplicate experiments are presented, error bars indicate s.d.

**Table 1** Inhibition of proliferation of several cell lines by GLP

| | *Cell lines* | | | | | | | |
|---|---|---|---|---|---|---|---|---|
| | *HMEC-1* | *HUVEC* | *NIH-3T3* | *MDA-MB-435* | *MKN-28* | *HCT-116* | *SK-OV-3* | *S-180* |
| $IC_{50}$ from 72 h exposure (mg ml$^{-1}$) | 0.86±0.34 | 0.64±0.24 | 1.01±0.13 | 1.77±0.36 | 1.66±0.16 | 1.42±0.19 | 2.65±0.53 | 1.72±0.24 |
| Inhibition of growth after 12 h exposure (%) | 4.60±1.20 | 8.52±2.21 | 6.56±1.32 | 3.71±1.52 | 6.49±2.49 | 3.50±0.57 | 5.52±0.92 | 2.57±1.17 |

The Table shows, in the upper row, the cytotoxic potential (as $IC_{50}$) of GLP, measured for a variety of cells after 72 h incubation with a range of concentrations (0.313–5 mg ml$^{-1}$). The lower row shows the effects of short-term incubation (12 h) with a relatively high concentration of GLP, about two to five times the $IC_{50}$. Under these conditions, cytotoxicity was always $<10\%$ and for some cell lines, $<5\%$. Values in the Table are the means±s.d. from three separate assays.

### *GLP inhibits HMEC-1 migration*

As endothelial cell migration is critical for the process of angiogenesis, we studied the effect of GLP on HMEC-1 migration *in vitro*. In our previous study (Tong *et al*., 2005), we found that an 8 h incubation time was optimal for HMEC-1 migration through the membrane from the upper to lower chambers, if the lower chamber contained MCDB131 culture medium supplemented with 20% FBS as a chemoattractant.

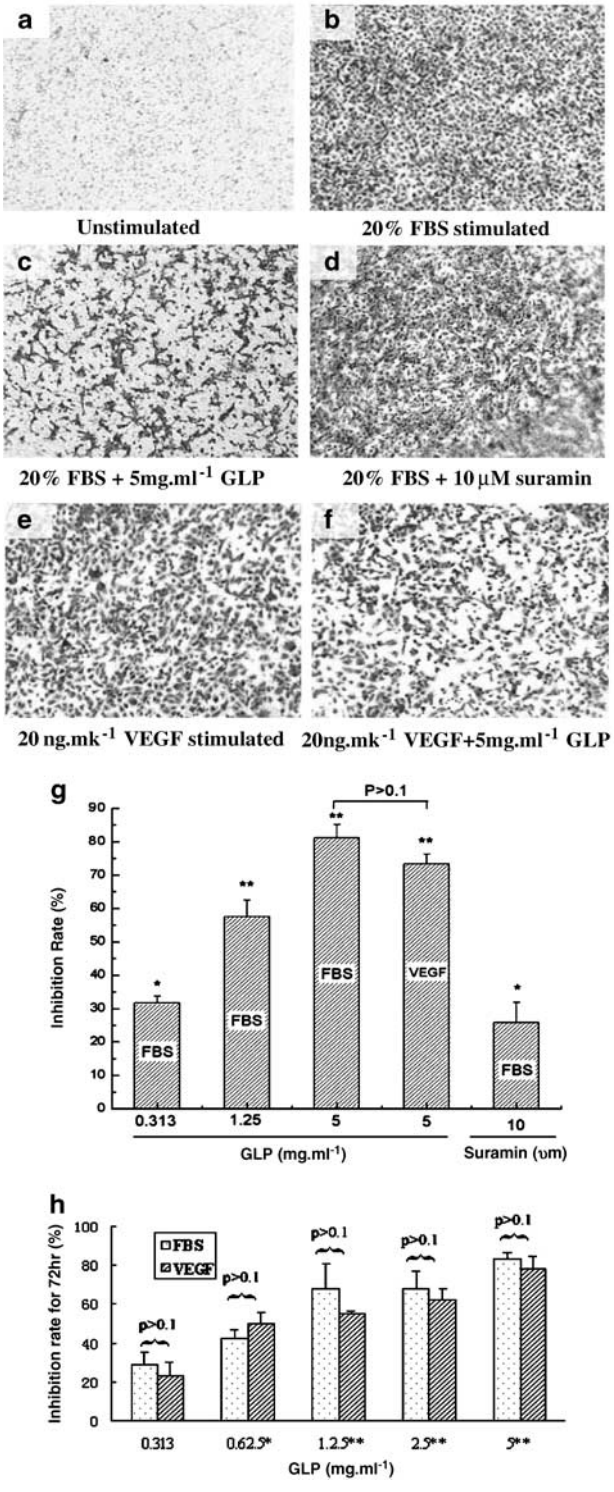


Here, we found that HMEC-1 migration was dose-dependently blocked by GLP (Figure 2a–c), with inhibition of 31.7, 57.5 and 81.1% at concentrations of 0.31, 1.25 and 5.0 mg ml$^{-1}$ GLP in normal culture conditions, respectively. In the same system, 10 $\mu$M suramin (positive control) inhibited 25.8% of cell migration (Figure 2d).

VEGF secreted by tumor cells is an important stimulus in tumor angiogenesis, especially for endothelial migration and proliferation. We compared the effects of GLP on HMEC-1 cell migration stimulated by VEGF or by 20% FBS. No detectable VEGF exists in FBS (VEGF ELISA, data not shown). VEGF (20 ng ml$^{-1}$) was less effective for HMEC-1 migration than FBS (Figure 2e), but 5.0 mg ml$^{-1}$ GLP blocked VEGF-stimulated migration of HMEC-1 cells (Figure 2f, 73.3% inhibition) as well as it inhibited migration due to 20% FBS (Figure 2g).

To assess effects of GLP on stimulated cell proliferation, HMEC-1 cells were starved overnight and proliferation induced by 20ng ml$^{-1}$ VEGF or 20% FBS. Various concentrations of GLP were tested against either stimulus. FBS had a more prominent ability to evoke HMEC-1 growth. After 72 h, the cells in the FBS control group were 2.5-fold greater than nonstimulated cells and the VEGF-stimulated control group were 1.9-fold greater than the nonstimulated cells. At every concentration of GLP, the proliferation of HMEC-1 cells stimulated by either stimulus showed similar inhibition (Figure 2h). So, GLP may not be a direct antagonist to VEGF-induced HMEC-1 migration and proliferation.

### *GLP inhibits HMEC-1 tube formation*

Capillary formation starts with endothelial cell differentiation and tube formation *in vitro* is also a consequence of endothelial cell differentiation. We tested whether GLP decreased the formation of tubes by HMEC-1 cells in Matrigel *in vitro*. Control HMEC-1 formed a mesh of tubes within 8 h (Figure 3a), whereas those treated with GLP did not. HMEC-1 treated with low concentrations (0.313 or 0.625 mg ml$^{-1}$) of GLP differentiated into short tubes but were unable to form meshes (Figure 3b), whereas those treated with higher concentrations (1.25, 2.5 and 5.0 mg ml$^{-1}$) remained dotted on the Matrigel without obvious morphological changes (Figure 3c). As mentioned above, treatment of HMEC-1 with 5 mg ml$^{-1}$ GLP for 12 h showed $<5\%$ inhibition of cell growth rate, indicating that the observed

**Figure 2** GLP blocked migration of HMEC-1 cells in Boyden chambers. The photographs show the lower chamber without chemoattractant (negative control, a); 20% FBS stimulated group (b); 5 mg ml$^{-1}$ GLP treated in 20% FBS (c); 10 $\mu$M suramin in 20% FBS (d); 20 ng ml$^{-1}$ VEGF stimulated group (e); 5 mg ml$^{-1}$ GLP treated with 20 ng ml$^{-1}$ VEGF (f). In (g) the experiments are summarized and the absorbance at 600 nm indicates the number of cells reaching the lower chamber. The inhibition was computed as $[1-(A_{600\ \text{treated}} \cdot A_{600\ \text{control}}{}^{-1})] \times 100\%$. Representative microscopic fields are shown. The mean of three independent experiments are presented, error bars indicate s.d. Magnification: 100-fold. $^*P<0.05$, $^{**}P<0.01$, GLP group vs control group, 20% FBS or 20 ng ml$^{-1}$ VEGF stimulated, respectively. In (h) inhibition by GLP of FBS or VEGF-stimulated HMEC-1 proliferation is compared. There was no difference between inhibition of these two stimuli over the entire dose range. $^*P<0.05$, $^{**}P<0.01$ GLP group vs control group, FBS- and VEGF-stimulated HMEC-1, respectively.

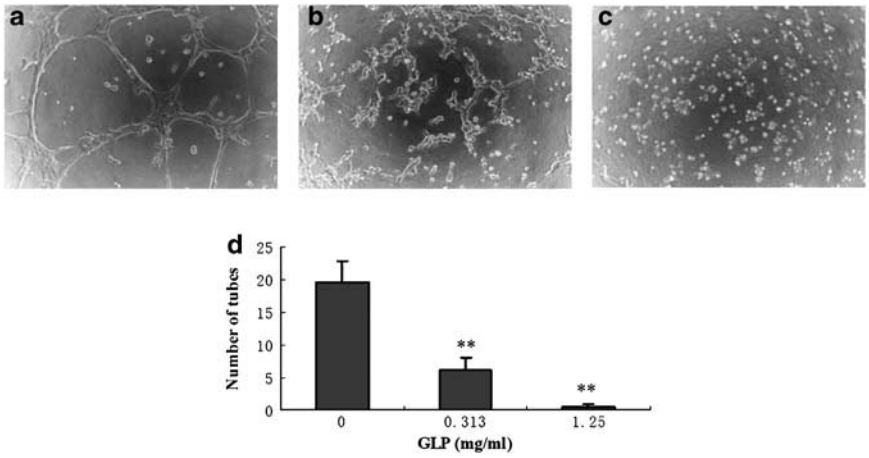


**Figure 3** GLP disrupted tube formation by HMEC-1 cells in Matrigel. HMEC-1 was seeded in Matrigel-coated 96-well plates. (a) HMEC-1 cells formed a complete mesh of tubes within 8 h on Matrigel. After treatment with GLP, cells stuck out short protrusions and aggregated into small masses (b, 0.313 mg ml$^{-1}$ GLP) or showed no differentiation morphology (c, 1.25 mg ml$^{-1}$ GLP). (d) In five random fields, tubes in enclosed networks were counted. The mean of three independent experiments are presented, error bars indicate standard deviation. Magnification: 40-fold. $^{**}P<0.01$, GLP group vs control group.

ability of GLP to inhibit tube formation was not due to cell growth inhibition.

### *GLP reduces neovascularization in a CAM assay*

The antiangiogenic activity of GLP was investigated *ex vivo* using a CAM assay, which is a convenient and reproducible test system for evaluating anti-angiogenic compounds. As shown in Figure 4a, control CAMs showed well-developed zones of neovascularization around and beneath the filter paper saturated with vehicle (buffered saline) after 2 days incubation. In contrast, CAM neovascularization was significantly suppressed by addition of GLP (2.5–50 $\mu$g egg$^{-1}$). Suramin (7.2 $\mu$g egg$^{-1}$), used as a positive control, is known to antagonize bFGF-induced angiogenesis. In our CAM assays, the number of vessel branches $<3$ mm long per unit area (see Methods) in each group were as follows: $13\pm2.2$ for control, $2\pm1.3$ for 2.5 $\mu$g egg$^{-1}$ GLP ($\sim2.5\times10^{-12}$ M, inhibition 84.6%), $4\pm1.6$ for 7.2 $\mu$g egg$^{-1}$ suramin ($5\times10^{-9}$ M, inhibition 69.2%). So, encouragingly, GLP showed more antiangiogenic activity, on a molar basis, than suramin.

### *GLP inhibits bFGF-induced angiogenesis in a Matrigel plug assay* in vivo

Matrigel plugs implanted in mice were used as the matrix for the growth of new vessels stimulated by bFGF. Dextran-FITC was injected to allow visualization of the vessels. In control plugs (GLP-free) removed from mice, angiogenesis was highly active and the main vessels showed frequent branching (Figure 5a). In contrast, GLP-treated plugs (0.5 mg plug$^{-1}$) showed narrower main vessels and fewer branches (Figure 5b). Quantitation of the fluorescence was carried out as described in the methods and the histogram analysis is illustrated in Figure 5c. Overall, GLP treatment lowered the angiogenic response compared to the control group. The percent fluorescence of GLP group ($n=5$) was $85\pm7.3$, while that of control group ($n=5$) was $47\pm6.9$ ($P<0.05$). Histograms showed that the peak shifted from green to black after GLP treatment.

### *GLP downregulates TF expression but without affecting VEGF cascades*

Since binding of VEGF to its receptors, flt-1 and KDR, is known to initiate angiogenesis, we looked for signs of GLP affecting the phosphorylation of these VEGF-receptors. Western blotting showed that GLP treatment did not significantly change the expression of pan-flt-1 and pan-KDR, nor did it change their phosphorylation levels greatly (Figure 6a). We then tested the response, to GLP exposure, of another cytokine, TF, which has been associated with angiogenesis in EGF- and VEGF-stimulated endothelial cells (Kaneko *et al*., 2003). Treatment of HMEC-1 cells with 0.2, 1.0 and 5.0 mg ml$^{-1}$ GLP for 24 h produced a dose-dependent decrease in TF mRNA copy number, as assessed by real-time RT–PCR (Figure 6b and c). Western blot analysis revealed that GLP treatment also decreased TF protein expression (Figure 6d) in these cells.

### *GLP inhibits tumor growth and tumor angiogenesis in mice bearing S-180 sarcoma cells*

Based on the antiangiogenic effects of GLP, we next measured the antitumor activity of GLP in female KM mice inoculated with S-180 sarcoma cells. Daily i.v. administration of 50, 100 or 200 mg kg$^{-1}$ GLP for 7 days yielded tumor inhibition of about 50% at the highest dose used (Table 2). Compared to the untreated tumor-bearing mice, the GLP-treated group did not lose weight greatly during the experiment, indicating that GLP has a relatively low toxicity. To clarify if the tumor inhibition was partially due to the antiangiogenic function of GLP, we assessed the vessel density and endothelial distribution in paraffin embedded sections of the tumor by immunofluorescence for CD 31. This protein, CD 31, is a specific endothelial and lymphocyte cell membrane marker (Albelda *et al*., 1991) and used here to identify the vessels and endothelial cells distribution in tumor sections. In the control group, many vascular branches grew out of a main vessel, the main vessels developed well and subvessels aligned very closely (Figure 7a). Also, many endothelial cells proliferated and

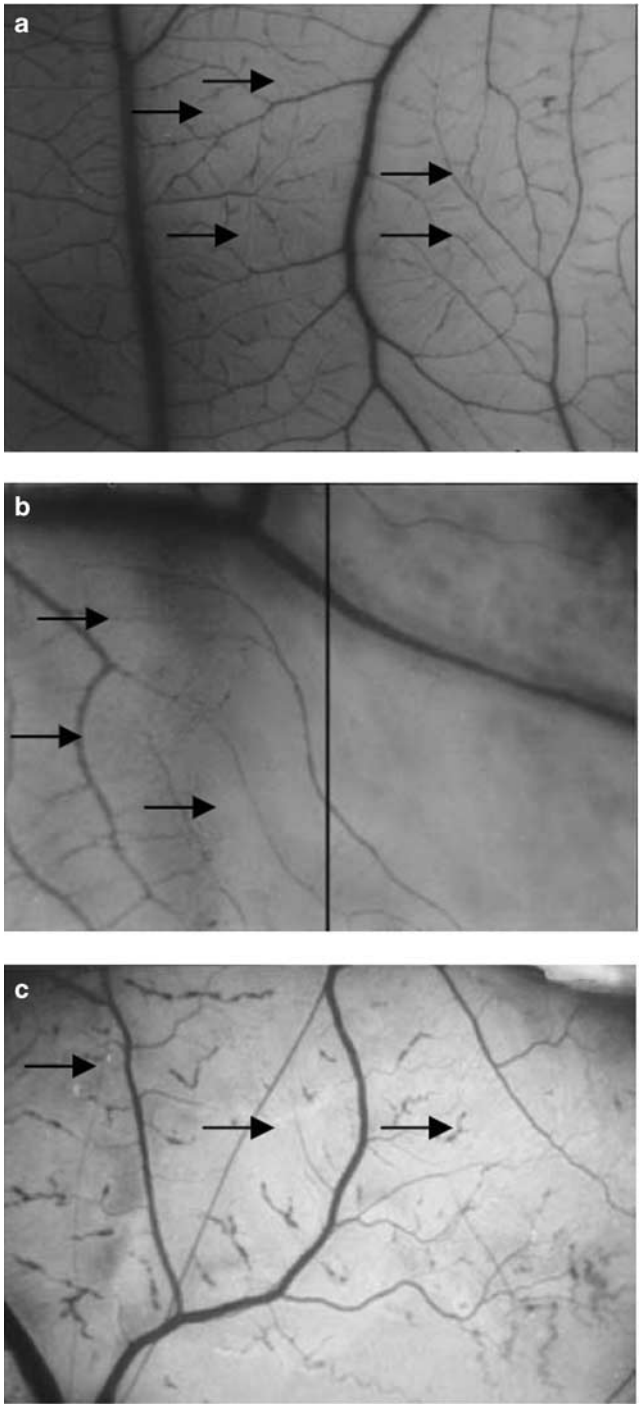


**Figure 4** Angiogenesis inhibited by GLP in CAM assay. (a) saline control, (b) CAM treated by GLP 2.5 $\mu g\,egg^{-1}$, or (c) suramin 7.2 $\mu g\,egg^{-1}$. In (b), the filter paper was placed on the right side of the field. **N**eovascularization on the left side was much stronger than the right side. The black line served as a borderline. Arrows show new vessels forming in CAM. Similar results were obtained from three independent experiments ($n=12$). Magnification: four-fold.

migrated from the vessels and were dotted around the vessels in transverse section (Figure 7c). After GLP treatment at 200 $mg\,kg^{-1}$ for 7 days, the main vessels in tumor sections did not form normal tube-like shapes, but developed constrictions and few branches grew out (Figure 7b); many fewer

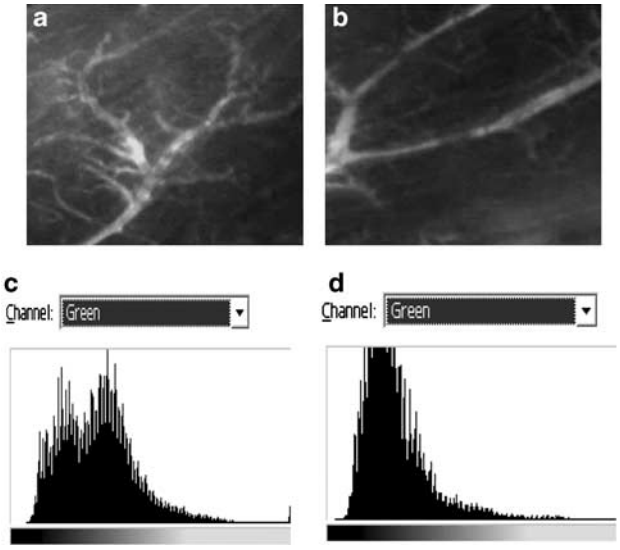


**Figure 5** GLP inhibited bFGF-induced angiogenesis in Matrigel plugs in mice. Dextran-FITC (green) outlined the vessel profiles. (a) In plugs without GLP, angiogenesis was highly active, with many newly formed vessels and many branches; (b) GLP decreased branches from main vessels. Magnification: four-fold. The 8-bit green band (fluorescence of FITC) was analyzed using Adobe® Photoshop® 7.0 (c for control group, d for treated group). $P<0.05$, GLP group vs control group. (For colour figure see online).

endothelial cells migrated from the 'mother' vessels (Figure 7d). These results strongly indicated that GLP was also exerting its antiangiogenic function *in vivo*. The percent fluorescence of GLP group (20 random fields from five mice) was $9.1\pm7.1$, while that of control group (20 random fields from five mice) was $25.2\pm6.3$. The inhibition was about 64%. Histograms showed that the peak shifted from green to black after GLP treatment.

## Discussion

A large variety of polysaccharide compounds from natural products have been found to possess multiple biological properties, including immune enhancement, stimulation of wound healing and anticancer functions. Recently, antiangiogenic activities have been increasingly reported in a number of polysaccharides from different sources, including pentosan polysulfate (a semisynthetic sulfated heparinoid polysaccharide; Lush *et al*., 1996), oversufhated fucoidan (Soeda *et al*., 2000), acharan sulfate (a new type of glycosaminoglycan from the giant African snail; Ghosh *et al*., 2002), and *G. lucidum* polysaccharides (Cao & Lin, 2004). All these have generated a surge of interest in development of polysaccharide-based antiangiogenesis and antitumor agents. Encouragingly, some are now under preclinical or even clinical studies.

Here, we report for the first time that GLP, a polysaccharide derived from marine alga, possesses distinct antiangiogenic activity. Noncytotoxic concentrations of GLP interfered with the key angiogenic steps of endothelial migration and tube formation. Treatment with 1.25 $mg\,ml^{-1}$ GLP inhibited migration of HMEC-1 cells by more than 50% and disrupted tube formation by these cells. *In vivo* assays revealed that GLP

($2.5\,\mu g\,egg^{-1}$) greatly inhibited the development of capillary networks in a CAM assay and lowered the density of neovascularization in Matrigel plugs implanted in mice.

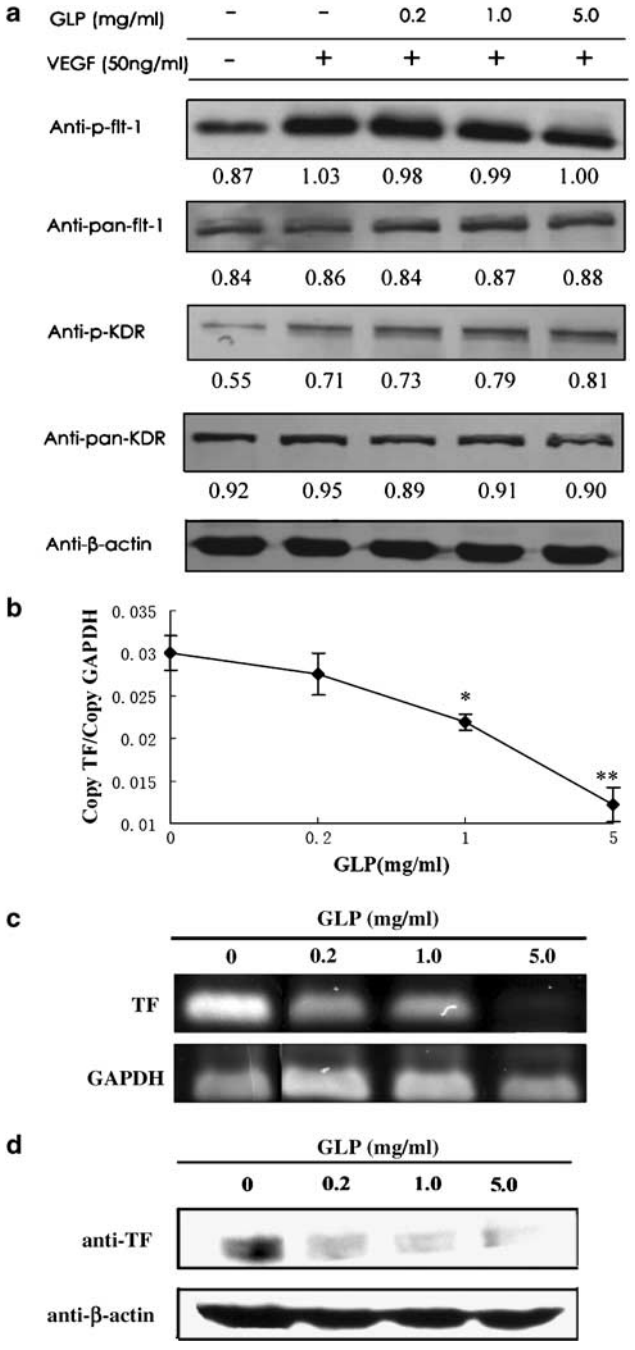


TF, a 47-KDa transmembrane glycoprotein, is an essential receptor for Factor VII/VIIa and is a primary initiator of blood coagulation *in vivo* (Edgington *et al*., 1991). TF treatment enhanced angiogenesis in bovine aorta endothelial cells, and this increased angiogenesis was inhibited by an anti-TF antibody (Watanabe *et al*., 1999). A recent study in mice using a cytoplasmic domain-deleted TF construct revealed that the TF/FVIIa complex promotes tumor and developmental angiogenesis through protease-activated receptor-2 (PAR-2) signaling independent of Factor Xa and other downstream proteases. Clotting-independent mechanisms of TF-induced tumor angiogenesis have also been described (Belting *et al*., 2004), mediated primarily by the cytoplasmic tail of the TF receptor. These papers suggest that TF could be a good target for new cancer therapeutics. In our present studies, we found that GLP treatment significantly decreased the mRNA and protein expression levels of TF in these cells, implying that the antiangiogenic actions of GLP involve a TF-dependent pathway.

There are many studies to describing correlations between TF and VEGF. Some reports showed that VEGF secreted by tumor cells may stimulate TF production (Abe *et al*., 1999) and in endothelial cell as well (Contrino *et al*., 1996). Others have indicated that TF and VEGF participate in a vicious cycle of clot formation in tumor growth. Aberrant expression of TF contributes to the angiogenic phenotype in part by upregulating expression of the proangiogenic growth factor, VEGF, and downregulating expression of the antiangiogenic protein, thrombospondin (Zhang *et al*., 1994). All these

**Figure 6** GLP treatment decreased TF expression without affecting phosphorylated and total flt-1 and KDR protein. In (a) After over-night starvation, HMEC-1 cells were treated with or without different concentrations of GLP for 2 h, and then stimulated by $50\,ng\,ml^{-1}$ VEGF. Total cell lysate was subjected to Western-blotting analysis. Antibodies against total and phosphorylated human flt-1 and KDR were used to visualize the protein expression and phosphorylation. The bands showed there was no change in either of the VEGF-receptors, including phosphorylated and total protein expression level after different concentrations of GLP. Densitometric analysis results are marked below each band and indicate the ratio of the band to that of $\beta$-actin. (b) Total mRNA of HMEC-1 isolated from cells with or without GLP treatment was subjected to semi-quantitative real-time PCR. This showed that the ratio between TF copy number and GAPDH copy number went down with increasing concentrations of GLP. GAPDH served as a standard gene whose mRNA was constant in various samples. Error bars indicate standard deviation, $^{*}P<0.05$, $^{**}P<0.01$, GLP group vs control group; In (c), the same results can be obtained from the 1.5% agarose gel electrophoresis image of the PCR products. The mean of triplicate experiments are presented, error bars indicate standard deviation; (d) Western blots showed a reduction in TF protein expression.

**Table 2** GLP inhibited tumour growth in mice implanted with S-180 sarcoma cells

| *Group* | *Dosage* ($mg\,kg^{-1}$) | *Means* | *Numbers* | | *Body weight* (g) | | *Tumor weight* (g) $x\pm s.d.$ | *Tumor inhibition (%)* | P-*value* |
|---|---|---|---|---|---|---|---|---|---|
| | | | *Begin* | *End* | *Begin* | *End* | | | |
| NS | — | | 16 | 16 | 21.5 | 31.5 | $1.17\pm0.14$ | — | — |
| GLP | 50 | i.v | 8 | 8 | 21.5 | 31.1 | $0.94\pm0.23$ | 19.4 | $>0.05$ |
| GLP | 100 | i.v | 8 | 8 | 21.5 | 30.4 | $0.87\pm0.17$ | 25.3 | $>0.05$ |
| GLP | 200 | i.v | 8 | 8 | 21.4 | 29.5 | $0.56\pm0.21$ | 52.1 | $<0.01$ |

Mice receieved S-180 cells and for the next 7 days were given a daily injection of saline (NS) or GLP, at the doses shown. Only at the highest dose was there a reduction in tumour weight after 7 days. Note that mice treated with GLP gained about the same weight as those treated with saline.

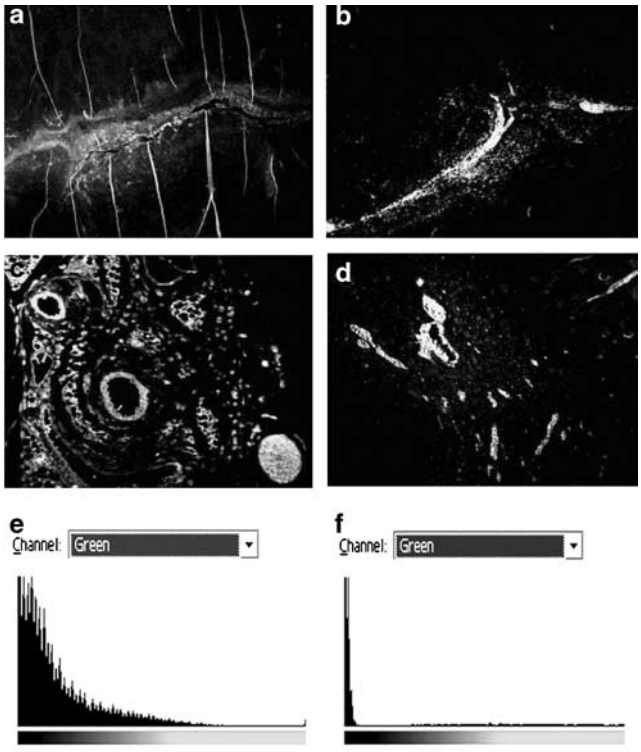


**Figure 7** GLP inhibited tumor angiogenesis in a mouse S-180 sarcoma model. Vessels in S-180 tumor sections were identified by anti-CD31 immunofluorescence and quantitated by Photoshop® histogram analysis. The fluorescent photographs show lower vessel densities in S-180 tumors after GLP treatment. In the control group, many branches were seen and differentiated into sub-branches (a, sagittal section, 40-fold amplification); many endothelial cells were in a highly active state of proliferation and migration from main vessels (c, transverse section, 100-fold amplification). However, in GLP-treated animals, the main vessels developed poorly and there was few branches (b, sagittal section, 40-fold amplification); endothelial cells seldom migrated far from the main vessel (d, transverse section, 100-fold amplification). Histogram analysis showed the green channel fluorescence, e (green channel percentage $25.2 \pm 6.3$) for control group, and f (green channel percentage $9.1 \pm 7.1$) for $200\,mg\,kg^{-1}$ GLP treated group. Each group included 20 different sections from 5 individual mice. Typical pictures are shown here. $P < 0.05$, GLP group vs control group.

considerations prompted us to hypothesize that TF was involved in the antiangiogenic effects of GLP as the result of cross-talk between VEGF and TF. However, in the current investigation, we found that there were no changes in either the protein levels or in the phosphorylation, of VEGFR1/2 following GLP treatment in HMEC-1 cells. From this we have inferred that inhibition by GLP of the angiogenic properties of HMEC-1 cells was independent of VEGF action.

Other antiangiogenic polysaccharides have been shown to act via effects on VEGF-VEGFR binding. Acharan sulfate inhibited VEGF-induced vascular tube formation, although this did not appear to be associated with decreased VEGF protein induction (Lee *et al*., 2003). *G. lucidum* polysaccharides isolated from the deep-layer cultivated mycelia of *Coriolus versicolor* also inhibited angiogenesis by interfering with VEGF-VEGFR activities (Cao & Lin, 2004). One reason for our present results to diverge from this general finding might be structural differences, in the sugar backbone and the extent and distribution of sulfate groups, but the detailed mechanism needs further study.

A previous study reported that pentosan polysulfate may be effective against breast carcinomas in which angiogenesis is due to tumor cell expression of FGFs (McLeskey *et al*., 1996). Another study reported a remarkable increase of lifespan in S-180 tumor-bearing mice treated with acharan sulfate (Lee *et al*., 2003). As GLP had antiangiogenic activities and direct effects on tumor cell proliferation *in vitro*, we further investigated the antitumor effect of GLP *in vivo*. Our experimental results showed that GLP potently inhibited tumor growth in a mouse sarcoma 180 model and induced a clear reduction of vessel density in tumors, However, the relationship between TF downregulation *in vitro* and anti-angiogenic activity *in vivo,* induced by GLP needs further detailed study.

This is the first study to demonstrate that the natural polysaccharide, GLP, acts as an inhibitor of angiogenesis, *in vitro* and *in vivo*. The mechanisms underlying its antiangiogenic and antitumor activities appear to involve the preferential targeting of TF. Taken together, our findings suggest that GLP would be beneficial in inhibiting tumor angiogenesis and tumor growth.

Grant sponsor: High Tech Research and Development Program; Grant number: 2002AA2Z346A, 2001AA624100; Grant sponsor: National Natural Science Foundation; Grant number: 30500649; the chemical section was supported by Shanghai Rising-Star Program, No. 03QD14048. The skillful technical assistance of Mr XI Yong and Mrs SHENG Hua is gratefully acknowledged.

## References

ABE, K., SHOJI, M., CHEN, J., BIERHAUS, A., DANAVE, I., MICKO, C., CASPER, K., DILLEHAY, D.L., NAWROTH, P.P. & RICKLES, F.R. (1999). Regulation of vascular endothelial growth factor production and angiogenesis by the cytoplasmic tail of tissue factor. *Proc. Natl. Acad. Sci. U.S.A.,* **96,** 8663–8668.

AKHTAR, N., DICKERSON, E.B. & AUERBACH, R. (2002). The sponge/Matrigel angiogenesis assay. *Angiogenesis,* **5,** 75–80.

ALBELDA, S.M., MULLER, W.A., BUCK, C.A. & NEWMAN, P.J. (1991). Molecular and cellular properties of PECAM-1 (endoCAM/CD31): a novel vascular cell-cell adhesion molecule. *J. Cell Biol.,* **114,** 1059–1068.

BELTING, M., DORRELL, M.I., SANDGREN, S., AGUILAR, E., AHAMED, J., DORFLEUTNER, A., CARMELIET, P., MUELLER, B.M., FRIEDLANDER, M. & RUF, W. (2004). Regulation of angiogenesis by tissue factor cytoplasmic domain signaling. *Nat. Med.,* **10,** 502–509.

BOUCK, N., STELLMACH, V. & HSU, S.C. (1996). How tumors become angiogenic. *Adv. Cancer Res.,* **69,** 135–174.

CAO, Q.Z. & LIN, Z.B. (2004). Antitumor and anti-angiogenic activity of *Ganoderma lucidum* polysaccharides peptide. *Acta. Pharmacol. Sin.,* **25,** 833–838.

CONTRINO, J., HAIR, G., KREUTZER, D.L. & RICKLES, F.R. (1996). *In situ* detection of tissue factor in vascular endothelial cells: correlation with the malignant phenotype of human breast disease. *Nat. Med.,* **2,** 209–215.

EDGINGTON, T.S., MACKMAN, N., BRAND, K. & RUF, W. (1991). The structural biology of expression and function of tissue factor. *Thromb. Haemost.,* **66,** 67–79.

FAHMY, R.G., DASS, C.R., SUN, L.Q., CHESTERMAN, C.N. & KHACHIGIAN, L.M. (2003). Transcription factor Egr-1 supports FGF-dependent angiogenesis during neovascularization and tumor growth. *Nat. Med.,* **9,** 1026–1032.

FOLKMAN, J. (1990). What is the evidence that tumors are angiogenesis dependent? *J. Natl. Cancer Inst.,* **82,** 4–6.

GHOSH, A.K., HIRASAWA, N., LEE, Y.S., KIM, Y.S., SHIN, K.H., RYU, N. & OHUCHI, K. (2002). Inhibition by acharan sulphate of angiogenesis in experimental inflammation models. *Br. J. Pharmacol.,* **137,** 441–448.

GUIRY, M.D. & NIC DHONNCHA, E. (2000). AlgaeBase. World Wide Web electronic publication, www.algaebase.org.

HANAHAN, D. & FOLKMAN, J. (1996). Patterns and emerging mechanisms of the angiogenic switch during tumorigenesis. *Cell,* **86,** 353–364.

HANAHAN, D. & WEINBERG, R.A. (2000). The hallmarks of cancer. *Cell,* **100,** 57–70.

HAWKER JR, J.R. (2003). Chemiluminescence-based BrdU ELISA to measure DNA synthesis. *J. Immunol. Methods,* **274,** 77–82.

KANEKO, T., FUJII, S., MATSUMOTO, A., GOTO, D., MAKITA, N., HAMADA, J., MORIUCHI, T. & KITABATAKE, A. (2003). Induction of tissue factor expression in endothelial cells by basic fibroblast growth factor and its modulation by fenofibric acid. *Thromb. J.,* **1,** 6.

KOS, M. & DABROWSKI, A. (2002). Tumour's angiogenesis—the function of VEGF and bFGF in colorectal cancer. *Ann. Univ. Mariae Curie Sklodowska [Med],* **57,** 556–561.

LEE, Y.S., YANG, H.O., SHIN, K.H., CHOI, H.S., JUNG, S.H., KIM, Y.M., OH, D.K., LINHARDT, R.J. & KIM, Y.S. (2003). Suppression of tumor growth by a new glycosaminoglycan isolated from the African giant snail Achatina fulica. *Eur. J. Pharmacol.,* **465,** 191–198.

LIOTTA, L.A., STEEG, P.S. & STETLER-STEVENSON, W.G. (1991). Cancer metastasis and angiogenesis: an imbalance of positive and negative regulation. *Cell,* **64,** 327–336.

LUSH, R.M., FIGG, W.D., PLUDA, J.M., BITTON, R., HEADLEE, D., KOHLER, D., REED, E., SARTOR, O. & COOPER, M.R. (1996). A phase I study of pentosan polysulfate sodium in patients with advanced malignancies. *Ann. Oncol.,* **7,** 939–944.

MCLESKEY, S.W., ZHANG, L., TROCK, B.J., KHARBANDA, S., LIU, Y., GOTTARDIS, M.M., LIPPMAN, M.E. & KERN, F.G. (1996). Effects of AGM-1470 and pentosan polysulphate on tumorigenicity and metastasis of FGF-transfected MCF-7 cells. *Br. J. Cancer,* **73,** 1053–1062.

NEUFELD, G., TESSLER, S., GITAY-GOREN, H., COHEN, T. & LEVI, B.Z. (1994). Vascular endothelial growth factor and its receptors. *Prog. Growth Factor Res.,* **5,** 89–97.

RICKLES, F.R., PATIERNO, S. & FERNANDEZ, P.M. (2003). Tissue factor, thrombin, and cancer. *Chest,* **124,** 58S–68S.

SHEU, J.R., FU, C.C., TSAI, M.L. & CHUNG, W.J. (1998). Effect of U-995, a potent shark cartilage-derived angiogenesis inhibitor, on anti-angiogenesis and anti-tumor activities. *Anticancer Res.,* **18,** 4435–4441.

SHIMIZU, T., KUBOTA, M., TANIZAWA, A., SANO, H., KASAI, Y., HASHIMOTO, H., AKIYAMA, Y. & MIKAWA, H. (1990). Inhibition of both etoposide-induced DNA fragmentation and activation of poly(ADP-ribose) synthesis by zinc ion. *Biochem. Biophys. Res. Commun.,* **169,** 1172–1177.

SOEDA, S., KOZAKO, T., IWATA, K. & SHIMENO, H. (2000). Oversulfated fucoidan inhibits the basic fibroblast growth factor-induced tube formation by human umbilical vein endothelial cells: its possible mechanism of action. *Biochim. Biophys. Acta.,* **1497,** 127–134.

TAN, W.F., LIN, L.P., LI, M.H., ZHANG, Y.X., TONG, Y.G., XIAO, D. & DING, J. (2003). Quercetin, a dietary-derived flavonoid, possesses antiangiogenic potential. *Eur. J. Pharmacol.,* **459,** 255–262.

TANAKA, N.G., SAKAMOTO, N., TOHGO, A., NISHIYAMA, Y. & OGAWA, H. (1986). Inhibitory effects of anti-angiogenic agents on neovascularization and growth of the chorioallantoic membrane (CAM). The possibility of a new CAM assay for angiogenesis inhibition. *Exp. Pathol.,* **30,** 143–150.

TONG, Y., ZHANG, X., TIAN, F., YI, Y., XU, Q., LI, L., TONG, L., LIN, L. & DING, J. (2005). Philinopside a, a novel marine-derived compound possessing dual anti-angiogenic and anti-tumor effects. *Int. J. Cancer,* **114,** 843–853.

WATANABE, T., YASUDA, M. & YAMAMOTO, T. (1999). Angiogenesis induced by tissue factor *in vitro* and *in vivo*. *Thromb. Res.,* **96,** 183–189.

ZHANG, Y., DENG, Y., LUTHER, T., MULLER, M., ZIEGLER, R., WALDHERR, R., STERN, D.M. & NAWROTH, P.P. (1994). Tissue factor controls the balance of angiogenic and antiangiogenic properties of tumor cells in mice. *J. Clin. Invest.,* **94,** 1320–1327.

*(Received November 15, 2005*
*Revised February 8, 2006*
*Accepted February 28, 2006*
*Published online 22 May 2006)*